Catal Lett (2009) 128:144–153
DOI 10.1007/s10562-008-9707-y

Evaluation of Foam Nickel for the Catalytic Partial Oxidation of Methane

L. J. I. Coleman · E. Croiset · W. Epling · M. Fowler · R. R. Hudgins

Received: 2 May 2008 / Accepted: 24 September 2008 / Published online: 26 November 2008

Abstract The catalytic activity of an industrially supplied nickel foam was evaluated for the conversion of methane to syngas via partial oxidation in air. At a temperature of 850 °C, 89% CH_4 conversion was attained with H_2 and CO selectivity of 96 and 97%, respectively. The catalytic performance of nickel foam was found to be comparable to an in-house prepared 10%wt Ni/γ-Al_2O_3. Interestingly the foam catalyst was found to be capable of light-off without in situ H_2 reduction unlike the supported nickel catalyst. CH_4 conversion and H_2 and CO selectivity were found to increase as the inlet temperature increased from 650 to 850 °C. Increasing the contact time by reducing the gas flow rate resulted in reduced CH_4 conversion and H_2 and CO selectivity, indicating substantial transport limitations. A key finding was that oxidative pretreatment of the nickel foam led to the formation of a surface oxide layer resulting in an increase in surface area and an improvement in catalytic activity.

Keywords Catalytic partial oxidation of methane · Metal foam · Nickel

L. J. I. Coleman · E. Croiset (✉) · W. Epling · M. Fowler · R. R. Hudgins
Department of Chemical Engineering, University of Waterloo, Waterloo, ON, Canada N2L 3G1
e-mail: ecroiset@uwaterloo.ca

Present Address:
L. J. I. Coleman
Center for Energy Technology, RTI International, Research Triangle Park, NC 27709-2194, USA
e-mail: lcoleman@rti.org

1 Introduction

Methane partial oxidation, reaction (1), although by no means a novel process [1], has recently become the focus of academic and industrial research as an attractive alternative to methane steam reforming [2]. The potential for energy savings and reduced capital investment for the production of syngas via the partial oxidation of methane is significant because of the absence of steam production, smaller reactor sizes, and the mild exothermicity of the reaction [2–9]. In addition, the H_2:CO ratio of 2:1 is more favorable for downstream processes such as methanol and Fischer–Tropsch synthesis [2, 3, 5]. These factors are major driving forces for further investigation.

$$CH_4 + \frac{1}{2}O_2 \leftrightarrow CO + 2H_2 \quad \Delta H^0_{298\,K} = -36\ \text{kJ mol}^{-1} \qquad (1)$$

Partial oxidation has not yet replaced steam reforming for several reasons. First, the reaction can easily 'run away' as a result of the formation of hot spots in the catalyst bed causing irreversible damage to the catalyst and raising serious safety concerns [5–7]. Also, the complete oxidation, reaction (2), being more exothermic than partial oxidation, has been found to occur simultaneously and can lead to enhanced 'run away' conditions [5].

$$CH_4 + 2O_2 \leftrightarrow CO_2 + 2H_2O \quad \Delta H^0_{298\,K} = -806\ \text{kJ mol}^{-1} \qquad (2)$$

Furthermore, the economics of the oxidation process depend on whether purified oxygen or air is used as the oxygen source. Oxygen purification significantly reduces the overall energy efficiency and profitability of the syngas production process. Alternatively, if air is used, the presence of N_2 in the product stream may adversely affect downstream processes. Finally, catalytic partial oxidation

reactions using supported-nickel catalysts typically deactivate via carbon deposition [6, 10–18], sintering [6, 10, 12, 13, 15–17, 19], solid-state transformations [9, 17, 20], and nickel volatilization through the formation of nickel carbonyls [20].

Two reaction pathways, direct and indirect, have been proposed to describe the methane partial oxidation reaction over supported catalysts [2, 6, 21–23]. The indirect pathway is a two-step process in which a portion of the methane undergoes complete combustion to H_2O and CO_2 with near complete consumption of oxygen. The combustion reaction is rapid and highly exothermic. Unconverted methane is subsequently dry (3) and steam (4) reformed to produce syngas, which generally approaches equilibrium via the water–gas shift reaction (5).

$$CH_4 + CO_2 \rightarrow 2H_2 + 2CO \quad (3)$$

$$CH_4 + H_2O \rightarrow 3H_2 + CO \quad (4)$$

$$CO + H_2O \leftrightarrow H_2 + CO_2 \quad (5)$$

In comparison to the complete oxidation reaction, the dry and steam reforming reactions are much slower and highly endothermic. Thus, the indirect pathway is characterized by an axial temperature profile that exhibits a strong exotherm at the entrance of the catalyst bed due to the highly exothermic combustion reaction followed by a rapid decrease in temperature caused by the endothermic reforming reactions [1, 2, 6, 11, 23]. In addition to the axial temperature profile, the indirect pathway leads to a catalyst composition profile. Dissanyake et al. [11] found that the catalyst bed, initially composed of Ni/α-Al_2O_3, could be separated into three zones during the partial oxidation of methane: $NiAl_2O_4$ + α-Al_2O_3, NiO/α-Al_2O_3, and Ni/α-Al_2O_3. The first two zones were found to be active for the complete oxidation of methane to CO_2 and H_2O, and the final zone, exposed to a reducing environment, was active for the reforming reactions producing H_2 and CO.

The direct reaction pathway is also a two-step process in which methane decomposes on the catalytic surface by either the pyrolysis, reaction (6), or the oxygen-assisted mechanism, reaction (7) [24].

$$CH_4 \rightarrow C^* + 4H^* \quad (6)$$

$$CH_x^* + (1 + x)O^* \leftrightarrow CO^* + xHO^* \quad (7)$$

On supported-nickel catalysts, pyrolysis (6) is the dominant direct reaction mechanism [23, 25, 26]. Differentiation of the dominant mechanism, whether direct or indirect, has been difficult to accomplish under most experimental conditions. High reaction temperatures inevitably lead to near-equilibrium conversions and product distributions even at low contact times and this is further complicated by the inclusion of strong heat and mass transfer effects [22]. Direct partial oxidation of methane is inherently faster resulting in reduced reactor volumes and more stable thermal profiles than the indirect. However, several research groups [2, 24] have shown that the indirect pathway gives higher conversion and more desirable H_2/CO ratios compared to the direct pathway.

Metallic foams are open-celled, highly porous, three-dimensional structures consisting of a network of solid strut polyhedral cells [27–31]. The physical and chemical properties (i.e., thermal and electrical conductivity, mechanical strength, melting point and corrosion resistance) of metallic foams are consistent with the source metal or alloy, while geometric properties such as pore size, strut diameter, and porosity are controlled during fabrication allowing the resulting foams a broad range of characteristics and applications. The highly porous, cellular structure gives the foam a high surface-to-volume ratio making them ideal mediums for depositing catalyst and catalyst support materials. The interconnectedness of the cellular structure yields a high cross-sectional flow area, resulting in a low-pressure drop while exhibiting enhanced gas–solid heat- and mass-transfer characteristics [27, 28]. Due to the high thermal conductivity of metallic foams, they are particularly well suited for reducing or eliminating localized hot- and cold-spot formation, leading to isothermal temperature profiles. Such unique properties have provoked interest in metallic foams as catalysts and catalyst supports for automotive applications [27, 28]. Metallic foams are generally used as support structures for high-surface-area ceramic supports such as γ-Al_2O_3 [26, 27, 31, 32]. However, very few studies have addressed the catalytic activity of the metallic foam itself. From those few studies, copper, copper alloys, nickel, nickel alloys [29, 30, 33], silver [33, 34], and ferrous alloys [31] foams have all shown catalytic activity for the oxidation of hydrocarbons.

In this study, the catalytic activity of nickel foam for the partial oxidation of methane was parametrically evaluated by investigating the effect of reaction temperature, gas flow rate, and bed depth on CH_4 conversion, H_2 and CO selectivity, and the H_2/CO molar yield ratio. In addition, the effect of an oxidative pretreatment on improving catalytic performance of the nickel foam was investigated by performing CH_4 decomposition on untreated and pre-oxidized nickel foam.

2 Experimental

2.1 Nickel Foam Wafers

Nickel foam wafers were prepared from INCOFoam® supplied by INCO Ltd. INCOFoam® is a pure nickel foam produced via a proprietary nickel carbonyl vapor deposition technique. It was supplied in sheets of 300 × 300 mm

and a mean thickness of 1.7 mm. The foam porosity was reported to be approximately 95% with a mean pore size distribution of 550–600 μm. Figure 1 shows the highly porous, open-celled, three-dimensional structure of the raw, untreated nickel foam wafer. Using a standard punch press, 9 mm diameter circular wafers having a thickness of 1.7 mm were formed each weighing approximately 50 mg. The bed depth was adjusted by changing the number of wafers stacked in series.

2.2 Methane Partial Oxidation

The catalytic activity of nickel foam for the partial oxidation of methane was evaluated using a conventional, down-flow, fixed-bed reactor test station consisting of a gas delivery system, fixed-bed reactor, reactor furnace, condenser, and product analyzer. Ultra-high purity methane (Praxair Inc.) and zero gas air (hydrocarbon-free, Praxair Inc.) were used as the reaction gases. The reactor was constructed from a 10 mm ID quartz tube with a highly porous quartz frit positioned such that the foam wafer would be located in the isothermal portion (i.e., within 2 °C) of the furnace. The foam wafer(s) were loaded on top of 1,000 mg of 35–50 mesh SiC (inert) resting on top of the quartz frit. The reaction temperature was monitored and controlled by a micro K-type thermocouple in a 3 mm OD quartz closed-ended sheath placed directly on top of and in contact with the nickel foam wafer. This temperature was used to control the furnace.

Once the nickel foam wafers were loaded into the reactor, the reactor temperature was ramped at 25 °C min^{-1} to the desired reaction temperature with flowing air at the desired rate required for the experiment. Once the target reaction temperature was reached, methane was added at a rate to provide a desired O_2/CH_4 mole ratio.

The product stream exiting the reactor passed through a water-chilled condenser to separate the condensable (water) and incondensable (H_2, O_2, N_2, CO, CH_4, and CO_2) species. An on-line Varian CP-3800 gas chromatograph (GC) was used to analyze the gaseous stream exiting the condenser. The GC was equipped with a thermal conductivity detector (TCD) and an $1/8'' \times 15'$, 60–80 mesh, Carboxen-1000 (Supelco Inc.) packed column. Since air was used as the oxygen source, the N_2 component was used as an internal standard to determine the flow rate of the product stream and aid in the evaluation of the carbon balance.

Definition of evaluation parameters:

$$\text{Methane conversion:} \quad X_{CH_4} = \frac{n^{in}_{CH_4} - n^{out}_{CH_4}}{n^{in}_{CH_4}} \cdot 100\% \tag{8}$$

$$H_2 \text{ Selectivity:} \quad S_{H_2} = \frac{n^{out}_{H_2}}{2\left(n^{in}_{CH_4} - n^{out}_{CH_4}\right)} \cdot 100\% \tag{9}$$

$$\text{CO Selectivity:} \quad S_{CO} = \frac{n^{out}_{CO}}{\left(n^{in}_{CH_4} - n^{out}_{CH_4}\right)} \cdot 100\% \tag{10}$$

$$H_2/CO \text{ molar yield ratio:} \quad H_2/CO = \frac{n^{out}_{H_2}}{n^{out}_{CO}} \tag{11}$$

where n_i^{in} and n_i^{out} represent the molar flow rates of the species i in and out of the reactor.

2.3 Characterization

Thermogravimetric analysis (TGA) was performed using a Cahn TG-2151 thermobalance equipped with electronic mass flow controllers, as previously described [35]. The initial sample mass of nickel foam used for all experiments was 50 mg. The sample temperature was elevated from room temperature to 850 °C at 10 °C min^{-1} with various dwell times at 850 °C. After each experiment the thermobalance was purged with N_2.

X-ray diffraction (XRD) patterns were collected by a Bruker AXS D8 Advance using standard Bragg–Brentano geometry with Ni-filtered Cu Kα radiation ($\lambda_1 = 1.5406$ Å, $\lambda_2 = 1.5444$ Å). Spectra were collected for a 2θ range of 10–100° using a step size of 0.05° and a count time of 1 s.

The surface area of the nickel foam samples was determined using a Micromeritics Gemini 3 2375 employing a multi-point BET analysis method. Samples were outgassed at 125 °C for 1 h in N_2. Anticipating that the nickel foam density and surface area would be very low, bulb sample tubes with filler rods were used and the equilibration time was extended to 30 s.

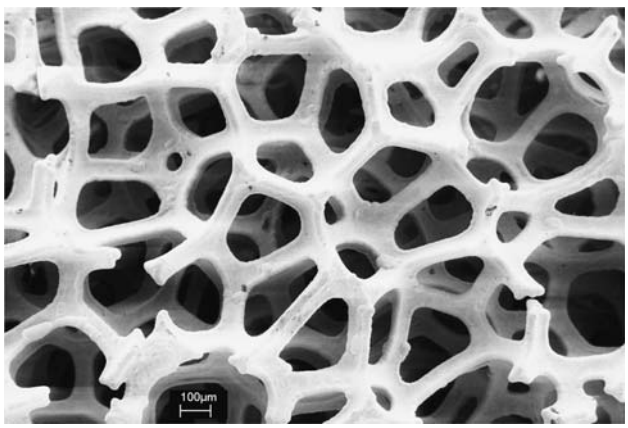

Fig. 1 SEM image showing the three-dimensional, highly interconnected cellular structure of the untreated "raw" nickel foam

3 Results and Discussion

The contribution of the reactor system, which consisted of SiC packing, quartz tube reactor, quartz-sheathed thermocouple,

and homogeneous gas phase reactions, to the conversion of methane was evaluated by performing blank experiments in the absence of nickel foam (catalyst) for all temperatures studied (650–850 °C). Methane conversion was found to be negligible for all temperatures studied verifying the inertness of the reactor system and the absence of homogeneous gas-phase reactions at the conditions studied.

All methane partial oxidation results presented in this manuscript represent the average performance over a 3 h period at the stated conditions. Equilibrium curves were obtained using the Gibbs' equilibrium reactor utility in Aspen Plus™ 12.1 (Aspen Technology, Inc.). The carbon balance for all partial oxidation reaction experiments was found to be within 98–102% indicating that very little carbon was deposited on the catalyst or reactor system and supports a high level of confidence in the analytical system.

3.1 Effect of Temperature

The effect of temperature is shown in Fig. 2 for (a) CH_4 conversion, (b) H_2 selectivity, (c) CO selectivity, and (d) the H_2/CO molar yield ratio for catalyst bed depths of 1.7 mm (one foam wafer) and 5.1 mm (three foam wafers loaded in series). Results obtained for 50 mg of an in-house prepared 10 wt% Ni/γ-Al_2O_3 catalyst are included for comparison. The effect of temperature was investigated using a total feed flow rate of 1,000 mL (STP) min^{-1} and an O_2/CH_4 molar feed ratio of 0.5 for temperatures between 650 and 850 °C. At 650 °C, the reaction took approximately 2 h to light-off after the introduction of methane. Light-off was indicated by a rapid rise in temperature and the immediate detection of syngas in the product gas. Prior to light-off, methane conversion was very low, approximately 3%, and CO_2 was the only product detected by the GC. No other oxidation/combustion products were detected most likely because of the insensitivity of the detector (TCD) to H_2 and water. The production of water was verified by the accumulation of a small amount of water in the quartz, water-chilled condenser at the reactor outlet. At 700 °C, the reaction took approximately 20 min to light-off and for reactions performed at 750, 800, and 850 °C, ignition was found to occur instantly upon the introduction of methane to the reactor feed. After light-off, no loss in catalyst activity was observed over the 3 h experiment. Increasing the reaction temperature resulted in increased CH_4 conversion and H_2 and CO selectivity even though oxygen had been completely consumed at temperatures as low as 650 °C. H_2 and CO were the main reaction products after ignition with selectivity ranging from 80 to 96% and 85 to 97%, respectively, for temperatures spanning 650–850 °C.

Temperature programmed reaction experiments, results not shown here, revealed that prior to ignition, the complete oxidation products, H_2O and CO_2, were the sole reaction products and CH_4 conversion was below 3%. However, upon ignition, which occurred at approximately 670 °C for an O_2/CH_4 feed ratio of 0.5, CH_4 conversion increased from 3% to greater than 50% almost instantly and the H_2 and CO selectivity increased from 0 to 65% and 78%, respectively. Upon ignition, the temperature of the catalyst rapidly rose from 670 to 763 °C in less than 1 min and returned to the set point after approximately 12 min. As the temperature continued to rise, due to the temperature ramp, CH_4 conversion and H_2 and CO selectivities

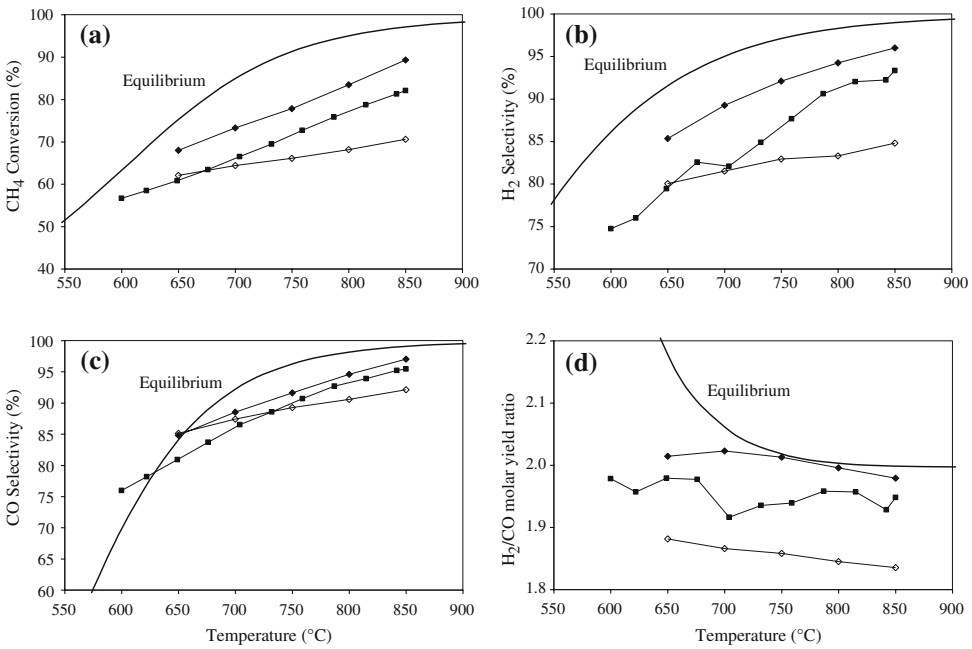

Fig. 2 Effect of temperature on **a** CH_4 conversion, **b** H_2 selectivity, **c** CO selectivity, and **d** H_2/CO molar yield ratio. Results are shown for one nickel foam wafer (◇), three nickel foam wafers (◆), and 10 wt% Ni/γ-Al_2O_3 (■)

steadily rose until the maximum temperature of the experiment (850 °C) was reached. The cooling portion of the temperature program revealed that the foam catalyst did not lose activity and the reaction did not extinguish at the ignition temperature of approximately 670 °C but instead extinguished between 610 and 635 °C.

From the results presented in Fig. 2, an increase in the foam bed depth from 1.7 to 5.1 mm yielded significant increases in all performance evaluation parameters. Because oxygen was completely consumed at all reaction temperatures for the 1.7 mm foam bed, above 650 °C, the greater conversion of CH_4 obtained with the 5.1 mm bed depth cannot be accounted for by oxidation reaction pathways. In addition, increasing the bed depth had a more significant effect on H_2 selectivity than on CO selectivity which is further demonstrated by the rise in the H_2/CO molar yield ratio with bed depth. The H_2/CO molar yield ratio, shown in Fig. 2d, decreased with increasing temperature suggesting that CO formation is more sensitive to the reaction temperature than the formation of H_2. These results suggest that the improved CH_4 conversion and H_2 and CO selectivity found for the 5.1 mm bed depth in the absence of oxygen is most likely related to the contribution of secondary reactions between methane and the complete combustion products H_2O and CO_2 via the steam (4) and dry (3) reforming of methane and the water–gas shift reaction (5).

3.2 Effect of Contact Time

The effect of contact time on the partial oxidation of methane was studied by two means; varying (1) the feed gas flow rate and (2) the bed depth (number of foam wafers). Manipulating the feed gas flow rate as a means of varying the contact time changes both the contact time and the flow conditions through the catalyst bed, resulting in changes to the heat- and mass-transfer characteristics of the system. Whereas, varying the contact time by changing the bed depth ensures similar heat- and mass-transfer characteristics between experiments. The effect of contact time was studied for feed gas flow rates ranging from 250 to 1,500 mL (STP) min^{-1} and nickel foam bed depths of 1.7 and 5.1 mm while the O_2/CH_4 molar feed ratio was maintained at 0.5. This corresponds to a range of contact times between 2.7 ms (low flow and 5.1 mm bed depth) and 0.14 ms (high flow and 1.7 mm bed depth). Contact time is defined as,

$$\tau = \frac{V_{\text{Foam}}}{F_{\text{T}}} = \frac{(1 - \varepsilon_{\text{Foam}})V_{\text{Wafer}}}{F_{\text{T}}} \tag{12}$$

where V_{Foam} is defined as the volume of the nickel foam excluding the void volume, $\varepsilon_{\text{Foam}}$ is the foam porosity, V_{Wafer} is the volume of the foam wafer, and F_{T} is the volumetric flow rate of the feed evaluated at the desired reaction temperature. The effect of contact time varied by manipulation of the gas flow rate on CH_4 conversion is given in Fig. 3. Oxygen conversion for all experimental conditions was 100% except for the experiment with the lowest space time of 0.14 ms at 700 °C which gave an oxygen conversion of 92.5%. As can be seen in Fig. 3, increasing the contact time by reducing the gas flow rate generally resulted in decreased CH_4 conversion. This result is counter-intuitive as increased contact time should result in increased CH_4 conversion. The observed relationship between contact time (flow rate) and conversion is indicative of significant transport limitations. Reynolds numbers, calculated using the strut diameter as the characteristic diameter, were found to be very low, ranging from 0.07 to 0.45 due to the extremely small diameter of the struts ($d_S \approx 6\times10^{-4}$ m, Fig. 1). Although several correlations have recently been proposed for predicting heat- and mass-transfer coefficients for metallic foams and meshes [27, 28], the calculated Reynolds numbers in this study are more than 100 times lower than the lower limits, which are typically Re = 10, for application of these correlations.

The presence of transport limitations is further supported by considering the results obtained for the effect of flow rate on CH_4 conversion and H_2/CO molar ratio at constant contact time given in Table 1. Increasing the gas flow rate, although having no effect on contact time due to the matched increase in bed depth, would increase the rate of heat- and mass-transfer between the flowing gas and the foam surface. Increased heat and mass transfer should only affect the conversion of a transfer-controlled reaction. In addition, the H_2/CO molar yield ratio increased with increasing contact time at all reaction temperatures indicating the increased role of the water–gas shift reaction.

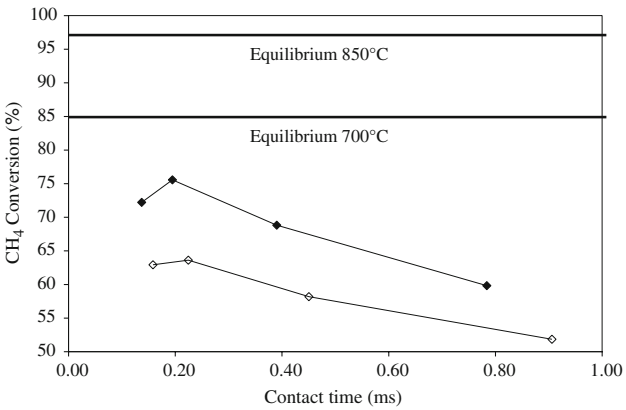

Fig. 3 Effect of contact time by manipulation of the gas flow rate on CH_4 conversion. Filled data points: 850 °C, Hollow data points: 700 °C

Table 1 Effect of flow rate on CH_4 conversion and H_2/CO molar ratio at constant contact time (~0.4 ms)

Temperature (°C)	Bed length (mm)	F_T (SmLPM)	CH_4 conv. (%)	H_2/CO (molar)
700	1.7	500	58.2	1.73
700	5.1	1,500	75.0	1.83
850	1.7	500	68.8	1.82
850	5.1	1,500	84.8	1.89

Results presented in Fig. 2 highlight the role of contact time under similar flow conditions. Increasing the contact time, while maintaining similar flow conditions, was achieved by increasing the nickel foam bed depth from 1.7 to 5.1 mm with a feed flow rate of 1,000 mL (STP) min^{-1}. For all temperatures investigated, it was found that increasing the bed depth improved CH_4 conversion and H_2 and CO selectivity.

3.3 Comparison to a Supported Nickel Catalyst

The catalytic performance of the nickel foam wafer catalyst was compared to an in-house prepared Ni/γ-Al_2O_3 catalyst. The supported nickel catalyst was prepared by wet impregnation of commercial γ-Al_2O_3 (Alfa-Aesar, 3 micron powder, 80–120 m^2 g^{-1}, 99.97% metal basis) with an aqueous nickel nitrate ($Ni(NO_3)_2 \cdot 6H_2O$) solution to give a 10 wt% Ni loading. The slurry was heated to 333 K and stirred to evaporate excess water. The resulting paste was dried overnight at 373 K, calcined at 1,023 K for 5 h, then crushed and sieved to collect the 35–45 mesh particles. The nickel content of the prepared Ni/γ-Al_2O_3 catalyst was determined to be 9.85 wt% by ICP analysis. XRD of the oxidized catalyst revealed the presence of γ-Al_2O_3, $NiAl_2O_4$, and NiO. XRD of the reduced catalyst identified only Ni and γ-Al_2O_3 and the mean nickel crystallite size was found to be 9.06 nm determined by application of the Scherrer equation to the Ni(200) peak. The BET surface area of the prepared Ni/γ-Al_2O_3 catalyst was 56.34 m^2 g^{-1}.

Experimental results comparing the performance of the nickel foam wafer and supported catalysts are presented in Fig. 2(a–d). The total amount of nickel present in each catalyst was 50 mg for one foam wafer, 150 mg for three foam wafers in series, and 5 mg for the 10 wt% Ni/γ-Al_2O_3 catalyst. To investigate the effect of in situ reduction on performance for the γ-Al_2O_3 supported Ni catalyst, temperature programmed reaction experiments, 450–850 °C at 1 °C min^{-1}, were performed on unreduced and reduced supported catalysts. The unreduced supported catalysts failed to light-off and produce syngas over the entire temperature range investigated, results not shown here. Small amounts of CH_4, less than 3%, were consumed and the only detectable reaction product was CO_2. CO_2 was detected in the product gas for reaction temperatures above 514 °C. The temperature for the onset of CO_2 production was significantly lower for the unreduced supported nickel catalyst than for the foam wafers. The supported catalyst, unlike the foam catalysts, required in situ hydrogen reduction prior to feeding the reaction mixture for the reaction to initiate and produce syngas.

The 10-wt% Ni/γ-Al_2O_3 catalyst was reduced in situ in 100 mL min^{-1} of 10% H_2 in N_2 at 750 °C for 1 h. After reduction, the temperature was reduced to 550 °C in N_2. A reaction gas mixture having an O_2/CH_4 ratio of 0.5 was fed at a rate of 1,000 mL (STP) min^{-1} to the reactor and the reaction lit-off instantly. Upon light-off, the temperature rise at the thermocouple was greater than 60 °C and the temperature of the catalyst bed could not be reduced below 600 °C. The temperature program was changed to ramp upward from 600 to 850 °C at a rate of 1 °C min^{-1}, and after 30 min at 850 °C the temperature was ramped downward to 450 °C at 1 °C min^{-1}. Similar to the foam wafer catalyst, CH_4 conversion, H_2 selectivity, and CO selectivity increased with increasing temperature. The performance of the supported catalyst fell consistently between one and three foam wafer values. During the cooling portion of the temperature program, the CH_4 conversion, H_2 selectivity, and CO selectivity were very similar to the ramp up results indicating no adverse effects from catalyst deactivation. However, the temperature of the catalyst bed could not be reduced below 588 °C even when the furnace temperature was below 200 °C. The reaction had become self-sustaining, a phenomenon not observed for the foam wafers.

3.4 Effect of Oxidative Pretreatment

Prior to the introduction of CH_4 to the feed mixture, the nickel foam wafers were preheated in air to the desired reaction temperature. SEM images of the strut surface for raw (Fig. 4) and pretreated, oxidized (Fig. 5) nickel foam samples reveal the effect of oxidative pretreatment on the surface morphology of the nickel foam. Exposure of the nickel foam wafer to an oxidative environment (air) at 850 °C for 30 min transformed the very smooth, flat surface of the raw sample to a highly irregular corrugated surface. The XRD pattern for the raw nickel foam sample, Fig. 6 (curve a), showed the presence of highly crystalline nickel. The oxidative pretreatment of nickel foam in air at 850 °C for 30 min, which will be discussed below, resulted in the oxidation of approximately 25% of the nickel to nickel oxide, and produced a surface layer of nickel oxide over the nickel core as shown in Fig. 6 (curve b). The result is a significant increase in surface area. The BET surface areas for raw and oxidized nickel foam samples were found to be 0.0432 and 0.1018 m^2 g^{-1} respectively. Interestingly,

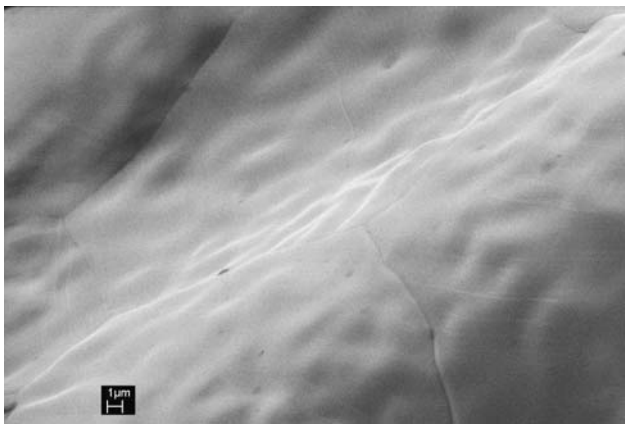

Fig. 4 SEM image of the surface of a strut for the untreated raw nickel foam

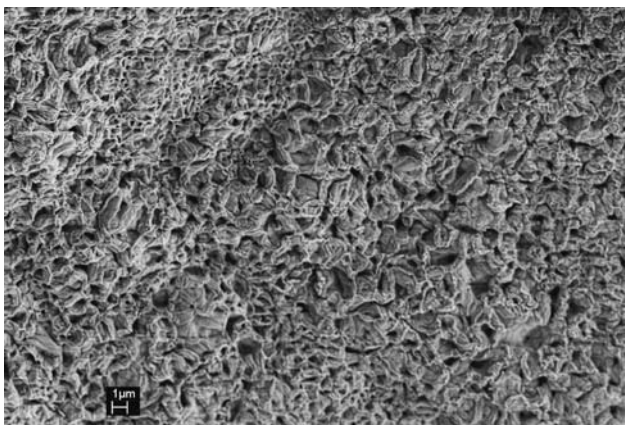

Fig. 5 SEM image of the surface of a strut for an oxidized nickel foam sample

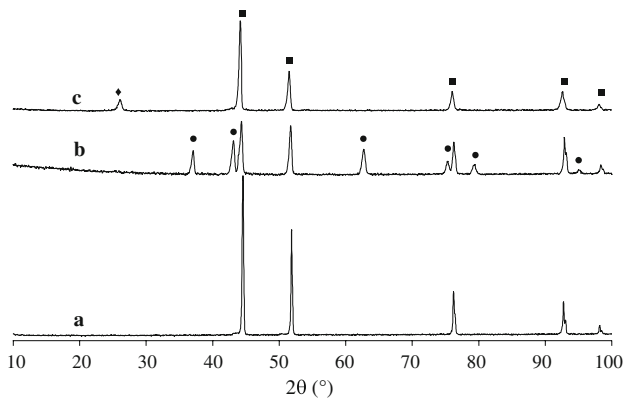

Fig. 6 XRD patterns for nickel foam under different treatments. Patterns: **a** raw nickel foam, **b** oxidized in air at 850 °C, and **c** oxidized nickel foam exposed to CH_4 at 850 °C. Crystalline species: nickel (■), nickel oxide (●), carbon (◆)

the irregular surface morphology of the oxidized sample was mostly retained after being exposed to methane partial oxidation reaction conditions at 850 °C for 8 h (Fig. 7).

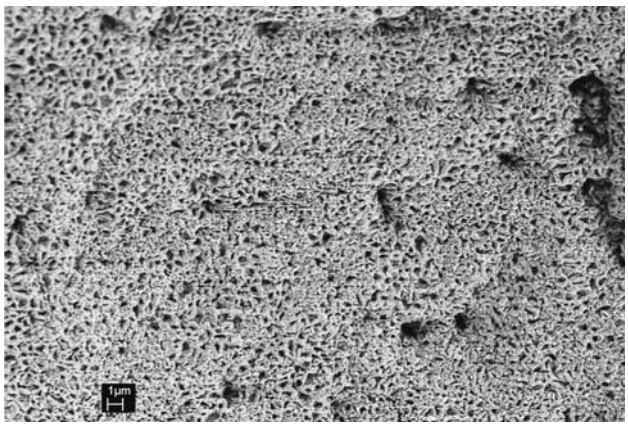

Fig. 7 SEM image of the surface of a strut for a nickel foam sample after methane partial oxidation

The effect of oxidative pretreatment on the catalytic activity of the nickel foam was investigated using a thermogravimetric technique. The decomposition of CH_4 to carbon and hydrogen, ($CH_4 \rightarrow C_s + 2H_2$), was selected as a model reaction for investigated since it has been identified as a primary reaction pathway in the indirect methane partial oxidation reaction network [36] and information on the reaction rate and onset can be measured gravimetrically [35]. This study assumes that the increase in weight is due solely to the deposition of carbon and not the adsorption of CH_4 or H_2. This is a reasonable assumption since the foams surface area is low (<0.1 m^2/g) and the temperatures investigated are high. Figure 8 presents weight gain (%) as a function of temperature for: (a) raw nickel foam with no oxidative pretreatment exposed to CH_4, (b) the oxidative pretreatment of nickel foam, and (c) oxidized nickel foam exposed to CH_4. The onset of weight gain for the raw nickel foam exposed to CH_4 occurred at approximately 803 °C and the rate of weight gain occurred very slowly (inferred from the slope) as shown in Fig. 8 (line a). Visual inspection of the sample upon removal from the TGA revealed that the sample had become blackened but had retained its original shape and structure. XRD revealed that the spent sample retained its original bulk crystal structure, Ni^0, and no crystalline carbonaceous structures were detected. XRD results are not presented for this sample in Fig. 6. These findings indicate that the methane decomposition reaction occurred only on the external surface of the nickel foam due to the low reactivity and the formation of a thin, most likely non-crystalline, carbonaceous layer.

As seen in Fig. 8 (line b) the onset of nickel foam oxidation occurred at 620 °C. The sample continued to gain weight resulting in a total weight gain of 26.9%. The theoretical weight gain for the complete oxidation of nickel to nickel oxide is 27.26%. The similarity between theoretical and experimental nickel oxidation weight gain

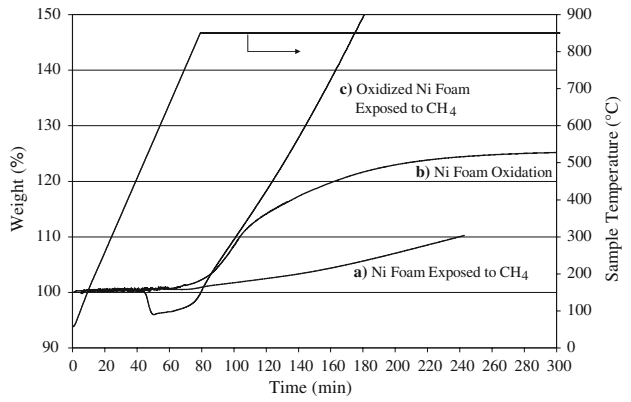

Fig. 8 Effect of oxidative pretreatment on nickel foam activity for CH_4 decomposition by TGA. Curve: **a** untreated nickel foam exposed to CH_4, **b** pretreatment of nickel foam with air, **c** oxidized nickel foam exposed to CH_4. Temperature program used for all experiments: 30–850 °C at 10 °C min^{-1} with various dwell times at 850 °C

indicates that the nickel foam sample had been completely oxidized to nickel oxide. Upon removal of the sample from the TGA it was apparent that the oxidized sample had experienced significant physical changes. The oxidized sample had changed color from metallic silver to green and the mechanical integrity had been severely compromised, becoming powder like.

Thermogravimetric analysis of partially oxidized nickel foam in CH_4 revealed several interesting features significantly different from raw nickel foam. The partially oxidized sample was prepared following the same procedure described for the fully oxidized sample except the partially oxidized sample was oxidized at 850 °C for 30 min, which resulted in approximately 25% of the nickel foam being oxidized to nickel oxide. The partially oxidized sample was then cooled to 30 °C in N_2, at which point CH_4 was admitted to the thermobalance and the temperature ramp was initiated. As shown in Fig. 8 (line c), the sample underwent rapid weight loss at approximately 480 °C, which is attributed to reduction of nickel oxide to metallic nickel. After losing approximately 5 wt%, which closely matched the weight gained during the oxidation stage, the sample weight stabilized and began to slowly increase. At approximately 670 °C, the rate of weight gain rapidly increased and continued until the sample gained in excess of 300% of its original weight after approximately 7 h at 850 °C. The effect of an oxidative pretreatment on nickel foam activity for the decomposition of methane was made obvious by comparison of the slopes of raw and partially oxidized nickel foam samples in Fig. 8. This result indicates that the oxidative pretreatment substantially improved the catalytic activity of the nickel foam for the decomposition of methane, which is the rate-limiting step for the methane partial oxidation reaction pathway [36]. XRD of this sample revealed that the surface nickel oxide produced during the oxidative pretreatment had been completely reduced to metallic nickel and the presence of carbon was observed.

3.5 Ignition Behavior

Supported nickel and nickel foam catalysts exhibited surprisingly different light-off behavior. The supported nickel catalyst, 10 wt% Ni/γ-Al_2O_3, was not able to light-off and produce syngas without in situ reduction in H_2. Several other studies [3, 8, 11, 36–38] found that in situ reduction with H_2 was not necessary for ignition to occur. In those studies, ignition was preceded by the oxidation of methane to CO_2 and H_2O with low CH_4 conversion. Of these studies, only the study by Dissanyake et al. [11] used nickel as the active catalyst phase and the nickel loading was quite high at 25% (reduced basis). To explain this ignition behavior, an Eley–Rideal-type reaction mechanism (13) was proposed to describe the interaction of gas phase methane with NiO as the route for the formation of CO_2 and H_2 [23].

$$CH_{4(g)} + 2NiO \rightarrow CO_{2(g)} + 2H_{2(g)} + 2Ni^0 \quad (13)$$

A reduced metal site is formed which can be re-oxidized to NiO by gas phase oxygen or adsorb CH_4. Since Ni^0 oxidation (14) occurs rapidly [23] and the concentration of oxygen is high, the reduced Ni site is most likely re-oxidized, therefore, no adsorption of methane and subsequent conversion to syngas occurs.

$$2Ni^0 + O_{2(g)} \rightarrow 2NiO \quad (14)$$

In addition, the activation energy for the desorption of oxygen is very high (464.4 kJ mol^{-1}) [22, 39] ensuring that the oxygen surface coverage remains near 100%.

Unlike unreduced supported nickel catalyst, oxidized nickel foam was able to convert methane to syngas without in situ reduction by H_2. Consider the experimental results at 650 °C. Initially, the foam catalyst gave the same performance as the unreduced supported catalysts; low methane conversion with 100% selectivity to CO_2. However, unlike the unreduced supported catalysts, after approximately 2 h of operation, the catalyst ignited and methane was converted to syngas. As the temperature of the reactor was elevated, the lag time for ignition decreased. For temperatures above 700 °C, ignition occurred instantly upon introduction of methane to the reactor.

In this study, the nickel foam catalyst was heated to the desired reaction temperature in a stream of air. This oxidative pretreatment created a thin layer of nickel oxide on the surface of the foam, as discussed above. At 650 and 700 °C, ignition and conversion of methane to syngas did not occur immediately upon the introduction of methane to the feed stream. The lag time for ignition decreased from

approximately 2 h at 650 °C to 20 min at 700 °C, and the consumption of oxygen occurred instantly for reaction temperatures of 750 °C and above. A possible mechanism for this ignition behavior could be related to the continued oxidation of the foam nickel in the presence of methane and oxygen. The assumption that nickel oxidation continued prior to ignition even in the presence of methane is consistent with the experimental data in that during this stage methane conversion was very low approximately 3%. The mechanism of nickel oxidation proposed by Chevalier et al. [40] can be described by two processes: (1) diffusion of Ni through the NiO scale and (2) diffusion of oxygen to the metal/metal oxide interface through cracks and fissures in the oxide scale. Cracking of the NiO scale would expose metallic nickel to the reaction gas and this newly exposed metallic nickel can either (1) be oxidized or (2) adsorb methane. The rate of Ni oxidation is rapid compared to the adsorption of methane [23]. The concentration of methane is higher than the O_2 concentration in the feed gas and the rate of methane diffusion through the NiO scale to the metal/metal oxide interface is faster as well, due to smaller molecular radius. This condition could lead to the adsorption of methane on metallic nickel sites, ultimately leading to the formation of hydrogen. The resulting hydrogen would reduce local NiO to metallic nickel at a much higher rate than methane further increasing the metallic site density and local temperature. This would increase the likelihood of methane adsorption resulting in ignition. At 650 and 700 °C, the oxidation process was slow and surface morphological changes occurred slowly, and therefore the exposure of metallic nickel to the reaction gas also occurred slowly resulting in lag times. For temperatures above 700 °C, conversion of methane to syngas occurred immediately upon the introduction of methane to the feed stream due to the increased rate of NiO scale formation and therefore increased access to metallic nickel. This would not occur for supported-nickel catalysts as the nickel crystallites would be completely oxidized during the calcination pretreatment and would therefore require in situ pre-reduction to become active for methane partial oxidation.

4 Conclusion

The catalytic performance of a nickel foam catalyst was evaluated for the production of syngas via the catalytic partial oxidation of methane. Nickel foam was found to be an active and selective catalyst achieving 89% methane conversion, 96% H_2 selectivity and 97% CO selectivity at 850 °C and performed comparably to a pre-reduced 10 wt% Ni/γ-Al_2O_3 catalyst. Unlike unreduced supported-nickel catalyst, the nickel foam catalyst was able to ignite the O_2/CH_4 mixture and produced syngas at temperatures as low as 650 °C without H_2 pre-reduction. The ability of the nickel foam to ignite the O_2/CH_4 mixture was attributed to the continuous growth of the nickel oxide layer on the foam strut, which resulted in the formation of cracks and fissures in the oxide layer exposing metallic nickel. The exposure of the metallic nickel sites was responsible for the ignition behavior of the foam catalyst. The steady state performance was found to be consistent with the results obtained for supported nickel catalysts.

Acknowledgments The authors gratefully acknowledge the financial support of this research by the Natural Sciences and Engineering Research Counsel of Canada (NSERC) and the Province of Ontario for funding LJIC in the form of an Ontario Graduate Scholarship (OGS). The authors would also like to acknowledge INCO Ltd. for supplying the INCOFoam® samples. The authors would also like to thank the reviewers for their thoroughly insightful comments which substantially improved the quality of this manuscript.

References

1. Prettre M, Eichner C, Perrin M (1946) The catalytic oxidation of methane to carbon monoxide and hydrogen. Trans Faraday Soc 42(3–4):335–340
2. Tsang SC, Claridge JB, Green MLH (1995) Recent advances in the conversion of methane to synthesis gas. Catal Today 23:3–15
3. Hickman DA, Schmidt LD (1993) Production of syngas by direct catalytic-oxidation of methane. Science 259:343–346
4. Hickman DA, Haupfear EA, Schmidt LD (1993) Synthesis gas formation by direct oxidation of methane over Rh monoliths. Catal Lett 17:223–237
5. Pena MA, Gomez JP, Fierro JLG (1996) New catalytic routes to syngas and hydrogen production. Appl Catal A Gen 144:7–57
6. York APE, Xiao T, Green MLH (2003) Brief overview of the partial oxidation of methane to synthesis gas. Top Catal 22:345–358
7. Reyes SC, Sinfelt JH, Feeley JS (2003) Evolution of processes for synthesis gas production: recent developments in an old technology. Ind Eng Chem Res 42:1588–1597
8. Eriksson S, Nilsson M, Boutonnet M, Jaras S (2005) Partial oxidation of methane over rhodium catalysts for power generation application. Catal Today 100:447–451
9. Song C, Pan W (2004) Tri-reforming of methane: a novel concept for catalytic production of industrially useful synthesis gas with desired H_2/CO ratios. Catal Today 98:463–484
10. Barbero J, Pena MA, Campos-Martin JM, Fierro JLG, Arias PL (2003) Support effect in supported Ni catalysts on their performance for methane partial oxidation. Catal Lett 87:211–218
11. Dissanyake D, Rosynek MP, Kharas KCC, Lunsford JH (1991) Partial oxidation of methane to carbon monoxide and hydrogen over a Ni/Al_2O_3 catalyst. J Catal 132:117–127
12. Basile F, Basini L, D'Amore M, Fornasari G, Guarinoni A, Matteuzzi D, Del Piero G, Trifiro F, Vaccari A (1998) Ni/Mg/Al anionic clay derived catalysts for the catalytic partial oxidation of methane—Residence time dependence of the reactivity features. J Catal 173:247–256
13. Chen L, Lu Y, Hong Q, Lin J, Dautzenberg FM (2005) Catalytic partial oxidation of methane to syngas over Ca-decorated-Al_2O_3-supported Ni and NiB catalysts. Appl Catal A Gen 292:295–304
14. Qin D, Lapszewicz J, Jiang X (1996) Comparison of partial oxidation and steam-CO_2 mixed reforming of CH_4 to syngas on MgO-supported metals. J Catal 159:140–149

15. Requies J, Cabrero MA, Barrio VL, Guemez MB, Cambra JF, Arias PL, Perez-Alonso FJ, Ojeda M, Pena MA, Fierro JLG (2005) Nickel/alumina catalysts modified by basic oxides for the production of synthesis gas by methane partial gas. Appl Catal A Gen 289:214–223
16. Xu S, Wang X (2005) Highly active and coking resistant $Ni/CeO_2–ZrO_2$ catalyst for partial oxidation of methane. Fuel 84:563–567
17. Yan QG, Weng WZ, Wan HL, Toghiani H, Toghiani RK, Pittman CU Jr (2003) Activation of methane to syngas over a Ni/TiO_2 catalyst. Appl Catal A Gen 239:43–58
18. Hu YH, Ruckenstein E (2002) Binary MgO-based solid solution catalysts for methane conversion to syngas. Catal Rev 44:423–453
19. Drago RS, Jurczyk K, Kob N, Bhattacharyya A, Masin J (1998) Partial oxidation of methane to syngas using NiO-supported catalysts. Catal Lett 51:177–181
20. Heitnes Hofstad K, Lindberg S, Rokstad OA, Holmen A (1994) Partial oxidation of methane to synthesis gas over a Pt/10% Rh gauze. Catal Today 21:471–480
21. Hickman DA, Schmidt LD (1992) Synthesis gas-formation by direct oxidation of methane over Pt monoliths. J Catal 138:267–282
22. Aghalayam P, Park YK, Vlachos DG (2000) Partial oxidation of light alkanes in short contact time microreactors. Catalysis 15:98–137
23. Vermeiren WJM, Blomsma E, Jacobs PA (1992) Catalytic and thermodynamic approach of the oxyreforming reaction of methane. Catal Today 13:427–436
24. Aghalayam P, Park YK, Fernandes N, Papavassiliou V, Mhadeshwar MB, Vlachos DG (2003) A C1 mechanism for methane oxidation on platinum. J Catal 213:23–38
25. Hu YH, Ruckenstein E (1995) Pulse-MS study of the partial oxidation of methane over Ni/La_2O_3 catalyst. Catal Lett 34:41–50
26. Hu YH, Ruckenstein E (1998) Isotopic GCMS study of the mechanism of methane partial oxidation to synthesis gas. J Phys Chem A 102:10568–10571
27. Giani L, Groppi G, Tronconi E (2005) Mass-transfer characterization of metallic foams as supports for structured catalysts. Ind Eng Chem Res 44(14):4993–5002
28. Giani L, Cristiani C, Groppi G, Tronconi E (2006) Washcoating method for Pd/-gamma-Al_2O_3 deposition on metallic foams. Appl Catal B Environ 62:121–131
29. Pestryakov AN, Fyodorov AA, Shurov VP, Gaisinovich MS, Fyodorova IV (1994) Foam metal catalysts with intermediate support for deep oxidation of hydrocarbons. React Kinet Catal Lett 53:347–352
30. Pestryakov AN, Fyodorov AA, Gaisinovich MS, Shurov VP, Fyodorova IV, Gubaydulina TA (1995) Metal-foam catalysts with supported active phase for deep oxidation of hydrocarbons. React Kinet Catal Lett 54:167–172
31. Shamsi A, Spivey JJ (2005) Partial oxidation of methane Ni–MgO catalysts supported on metal foams. Ind Eng Chem Res 44(19):7298–7305
32. Chin P, Sun X, Roberts GW, Spivey JJ (2006) Preferential oxidation of carbon monoxide with iron-promoted platinum catalysts supported on metal foams. Appl Catal A Gen 302:22–31
33. Pestryakov AN, Lunin VV, Devochkin AN, Petrov LA, Bogdanchikova NE, Petranovskii VP (2002) Selective oxidation of alcohols over foam-metal catalysts. Appl Catal A Gen 227:125–130
34. Pestryakov AN, Lunin VV, Bogdanchikova NE, Petranovskii VP, Knop-Gericke A (2003) Supported foam-silver catalysts for alcohol partial oxidation. Catal Commun 4:327–331
35. Rahman MS, Croiset E, Hudgins RR (2006) Catalytic decomposition of methane for hydrogen production. Top Catal 37:137–145
36. Wei J, Iglesia E (2004) Isotopic and kinetic assessment of the mechanism of reactions of CH_4 with CO_2 or H_2O to form synthesis gas and carbon on nickel catalysts. J Catal 224:370–383
37. Mallens EPJ, Hoebink JHBJ, Marin GB (1995) An investigation on the reaction mechanism for the partial oxidation of methane to synthesis gas over platinum. Catal Lett 33:291–304
38. Mallens EPJ, Hoebink JHBJ, Marin GB (1997) The reaction mechanism of the partial oxidation of methane to synthesis gas: a transient kinetic study over rhodium and a comparison with platinum. J Catal 167:43–56
39. Hei MJ, Chen HB, Yi J, Lin YJ, Lin YZ, Wei G, Liao DW (1998) CO_2-reforming of methane on transition metal surfaces. Surf Sci 417:82–96
40. Chevalier S, Desserrey F, Larpin JP (2005) Oxygen transport during the high temperature oxidation of pure nickel. Oxid Metals 64:219–234